Ligand Binding to the Membrane-Bound Acetylcholine Receptor from *Torpedo marmorata*: A Complete Mathematical Analysis†

Heino Prinz‡ and Alfred Maelicke*,§

Max-Planck-Institut für Ernährungsphysiologie, Rheinlanddamm 201, D-4600 Dortmund, Germany, and Institut für Physiologische Chemie der Johannes-Gutenberg Universität, Duesbergweg 6, D-6500 Mainz, Germany

Received August 20, 1991; Revised Manuscript Received April 15, 1992

ABSTRACT: We have studied by means of equilibrium binding and kinetic experiments the interaction of the membrane-bound nicotinic acetylcholine receptor (nAChR) from *Torpedo marmorata* with [^{3}H]acetylcholine and the fluorescent agonist NBD-5-acylcholine. In agreement with previous studies by others, we observed the preexistence, in the absence of ligand, of an equilibrium between two states of the nAChR, one with high affinity and the other with low affinity for agonist. As additional requirements for a minimal reaction scheme, we recognized (i) the existence of two ligand-binding sites, each of which may exist in two conformational states when occupied, and (ii) ligand-induced transitions between these conformations. Employing a special form of the allosteric model which considers these requirements, we then developed a suitable algorithm in order to simultaneously fit the whole set of equilibrium binding and kinetic data obtained for the two ligands. In this way we determined for a minimal model of the mechanism of action of the nAChR the complete set of rate constants and K_D values involved. With these values available, we were able to simulate the rise and fall in the concentrations of individual receptor–ligand complexes and conformations occurring in the course of excitatory events at the electrocyte synapse. The membrane environment of the nAChR plays a decisive role with respect to the rates of conformational change of the nAChR occurring in the course of ligand interaction. Thus, artificial changes in membrane structure and composition can speed up by several orders of magnitude the rate of conformational change ("desensitization"). A proper structure of the surrounding membrane hence is a prerequisite for the physiological function of the membrane-embedded nAChR.

A large body of equilibrium binding studies has established the existence of two cooperatively interacting binding sites for ACh[1] at the membrane-bound nAChR (Neubig & Cohen, 1979; Fels et al., 1982). The two binding sites are nonequivalent (Weber & Changeux, 1974a; Maelicke et al., 1977; Neubig & Changeux, 1979, 1980; Kang & Maelicke, 1980; Watters & Maelicke, 1983; Prinz & Maelicke, 1983a; Covarrubias et al., 1986) although the α-subunits are encoded by a single gene (Merlie et al., 1983; Klarsfeld et al., 1984) and hence are probably identical in primary structure.

Previous electrophysiological and biochemical studies have been analyzed by a four-state concerted model of allosteric interactions (Changeux & Podleski, 1968; Changeux et al., 1988) assuming one resting, one active (open channel), and two desensitized states. The equilibrium between these states, which preexists in the absence of ligand (Monod et al., 1965; Changeux & Podleski, 1968; Heidmann & Changeux, 1979, 1980; Neubig et al., 1982; Sine & Taylor, 1982; Jackson, 1984; Steinbach et al., 1986), is shifted upon ligand binding, giving rise to the various patterns of activity detected by electrophysiological and ion flux studies (Auerbach & Sachs, 1983; Covarrubias et al., 1984; Colquhoun & Ogden, 1986; Steinbach, 1989; Sine et al., 1990). The existence of different conformational states of the nAChR has been shown by conformation-sensitive proves (Heidmann & Changeux, 1979, 1980; Prinz & Maelicke, 1983a,b; Covarrubias et al., 1986). Likewise, ligand-induced transitions between such states are well established (Dunn et al., 1980, 1989; Prinz & Maelicke, 1983b). Ligand binding to the nAChR is an entropy-driven process (Maelicke et al., 1977) involving conformational adjustments of receptor and ligand (Dunn et al., 1980; Kang & Maelicke, 1980; Pearce & Hawrot, 1990; Conti-Tronconi et al., 1991) and long-range allosteric coupling between functional domains (McCarthy & Stroud, 1989).

From time-resolved ligand-binding and ion flux studies (Weber & Changeux, 1974b; Sine & Taylor, 1979; Dunn et al., 1980; Heidmann & Changeux, 1979; Boyd & Cohen, 1980), the majority of *Torpedo* nAChR molecules in the native membrane environment preexists in a state which binds agonist with low affinity ("resting" state). Prolonged exposure of the receptor to agonist leads to a conformational transition to state(s) of high affinity of agonist binding while the affinity for antagonist is changed only insignificantly, if at all. Two rates of affinity increase for agonist have been resolved (Neubig et al., 1982; Heidmann et al., 1983; Karpen et al., 1983) and correlate well with the time courses of electrophysiological desensitization (Katz & Thesleff, 1957; Fels et al., 1982), suggesting that the two phenomena are related to each other. This is further supported by the effects of local anesthetics and organic solvents which increase both the rate of affinity increase for agonist (Weiland & Taylor, 1979; Boyd & Cohen, 1984) and the rate of desensitization (Ogden et al., 1981).

Notwithstanding the large body of experimental binding and kinetic data available, their complete mathematical

† This work was supported by Grant Ma 599/9 of the Deutsche Forschungsgemeinschaft and a grant to A.M. of the Fonds der Chemischen Industrie.

* Author to whom correspondence should be addressed.

‡ Max-Planck-Institut für Ernährungsphysiologie.

§ Institut für Physiologische Chemie der Johannes-Gutenberg Universität.

[1] Abbreviations: A_2C, 2-(2-methoxyethoxy)ethyl-8-(*cis*-2-*n*-octylcyclopropyl)octanoate; NBD-5-acylcholine, *N*-(7-nitro-2,1,3-benzoxadiazol-4-yl)-5-aminopentanoic acid β-(*N,N,N*-trimethylammonium) ethyl ester; ACh, acetylcholine; nAChR, nicotinic acetylcholine receptor; Tetram, *S*-(2,2-diethylamino)ethylphosphorothioic acid *O,O*-diethyl ester; TMF, *Torpedo* membrane fragments.

0006-2960/92/0431-6728$03.00/0

Scheme I

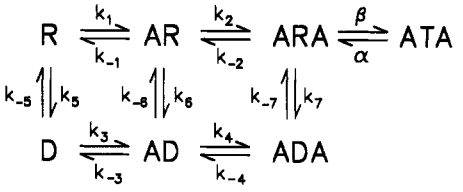

analysis has not yet been seriously attempted. This is largely due to the fact that even the simplest models conforming with the above-mentioned properties of nAChR–ligand interaction (Neubig & Cohen, 1980; Fong & McNamee, 1986; Delcour & Hess, 1986) involve a considerable number of reaction steps (Scheme I) and the related rate and equilibrium constants.

Scheme I contains 16 rate constants and, if fluorescence signals are to be monitored, in addition at least five fluorescence quantum yields, i.e., a minimum of 21 unknown parameters. This formidable number of parameters certainly cannot be determined reliably by classical fitting procedures of a limited data set, e.g., singular rapid kinetic experiments. Instead, several sets of independent data together with a good numerical fitting procedure and a carefully designed streategy of parameter reduction and initial values selection is required to achieve a consistent set of parameters of reasonable confidence. In the present work, we have engaged in this task because we feel that the availability of a complete set of rate and equilibrium constants may help to answer some of the central but still unsolved questions related to the mechanism of action of the nAChR.

The initial values of rate and equilibrium constants employed in the fitting procedure came from three sources, i.e., electrophysiological data (Sine & Steinbach, 1987), equilibrium binding data employing radioactively labeled ACh, and time-resolved kinetics employing radioactively labeled ACh and/or the fluorescent agonist NBD-5-acylcholine. The equilibrium binding and kinetic studies were performed under identical experimental conditions and were analyzed at two levels, conventional curve fitting in order to obtain rough values for some equilibrium and rate constants and simultaneous numberical fitting of Scheme I in order to obtain a complete set of all parameters involved. In a preceding study (which is described at the beginning of Results), the applicability of Scheme I as a model for the receptor's mechanism of ligand interaction was scrutinized. Taken together, this approach yielded a set of parameters that (i) is in agreement with the results of most previous experimental studies and (ii) expands these to a new level of quantification which for the first time permits the mathematical simulation of excitation–inactivation cycles at the cholinergic synapse.

MATERIALS AND METHODS

[^{3}H]Acetylcholine and [^{3}H]tubocurarine were obtained from Amersham, Braunschweig, Germany. Contamination of radioactive ligand with nonbinding radioactivity (between 9% and 17% of total radioactivity) was determined for each batch by counting the remaining radioactivity in the supernatant after repeated centrifugation with an excess of receptor. HEPES, PIPES, bovine serum albumin, α-bungarotoxin, acetylcholine, and tubocurarine were purchased from Sigma, München, Germany. All standard chemicals including carbamoylcholine were obtained from Merck, Darmstadt, Germany. All binding and kinetic studies were performed under identical buffer conditions, i.e., in "standard buffer": 100 mM NaCl, 4 mM $CaCl_2$, 2 mM $MgCl_2$, and 10 mM PIPES, pH 6.8.

Live electric rays, *Torpedo marmorata*, were obtained from the Station Biologique d'Arcachon, France. Two different preparations were used and compared in our studies. (i) Electric rays were transported live in our laboratory and their electric organs dissected immediately prior to the preparation of membrane-bound nAChR. (ii) Electric organs were dissected in Arcachon and immediately frozen in liquid nitrogen. This material was transported and stored (up to 1 year) under liquid nitrogen until used. When both preparations were compared, no difference in properties was detected in either equilibrium binding or kinetic studies.

nAChR-Rich Torpedo Membrane Fragments (TMF). Approximately 20 g of freshly dissected or frozen electric tissue was homogenized at 40 000 rpm for 6 × 15 in four volumes of 0.1 M NaCl, 0.02 M HEPES, 2 mM $MgCl_2$, and 2 mM $CaCl_2$, pH 7.4, using a Virtis homogenizer. The homogenate was filtered through two layers of cellulose filter cloth and centrifuged at 48000g for 60 min. Membrane fragments were partially purified according to Fels et al. (1982) using the following buffer conditions for the repeated centrifugation steps: 5 mM EDTA, 10 mM sodium azide, 0.21 mg/mL phenylmethanesulfonyl fluoride (PMSF), and 1.3 mg/mL iodoacetamide in 10 mM sodium phosphate buffer, pH 7.4. The final pellet was then resuspended in "standard buffer" (see above). The concentration of acetylcholine binding sites was determined for each preparation by extrapolation of an equilibrium binding curve obtained with [^{3}H]acetylcholine and the centrifugation assay previously described (Prinz & Veltel, 1986).

Rapid Filtration Assay. Filtrations were performed by means of a Millipore filtration unit no. XX2702550 (Millipore Corp., Bedford, MA) employing Whatman GF/C filters. Prior to each experiment, the filters were pretreated with 200 μL of standard buffer. The reaction was started by mixing the indicated concentrations of [^{3}H]acetylcholine or [^{3}H]tubocurarine in standard buffer with a solution of *Torpedo* membrane fragments (TMF) containing the anticholinesterase inhibitor Tetram (10 mM) in standard buffer. The reaction volume was 15 mL, of which 1 mL was filtered at each indicated time point. Because of spontaneous aerosol formation during filtration, the volume of the filtrate did not remain constant. Therefore, the concentration of free ligand was determined from the radioactivity of aliquots (3 × 150 μL) of the filtrate. The radioactivity corresponding to the total ligand concentration (free ligand concentration at zero time) was determined by taking a 1-mL aliquot from the original solution of 15 mL, adding 10 μL of 0.1 M nonradioactive acetylcholine (or tubocurarine), and filtering by the same procedure as described above. In the case of the fluorescent agonist NBD-5-acylcholine, the ligand concentrations were determined by quantitative fluorescence analysis employing a SLM 8000 photon-counting fluorimeter (SLM, Urbana, IL). $C_B(t)$, the concentration of bound ligand at a given time, was calculated from the known total ligand concentration C_0, its corresponding radioactivity (or fluorescence) CPM_0, and the radioactivity (or fluorescence) in the filtrate $CPM(t)$:

$$C_B(t) = C_0 - \frac{CPM(t)C_0}{CPM_0} \quad (1)$$

Fluorescence Kinetics. The fluorescent agonist NBD-5-acylcholine (Jürss et al., 1979; Meyers et al., 1983) was employed as monitoring ligand. The kinetics were performed in a Durrum stopped-flow spectrometer (series D-100) with a fluorescence attachment. A continuous argon laser (Spectra-

Physics 164-03) tuned to 488 nm served as the light source. The data were sampled, averaged, and calibrated as described in detail elsewhere (Prinz & Maelicke, 1983b). When used for simultaneous numerical fits, the number of points was further reduced, achieving an even distribution of a logarithmic time scale. All fluorescence kinetic experiments were performed in standard buffer at 22 °C.

Extended Data Analysis (Simultaneous Fits). Extended data analysis was performed with the program FACSIMILE (United Kingdom Atomic Energy Authority, 1986). The program permits the numerical solution of differential equations corresponding to different reaction schemes. It requires initial estimates of all parameters to be fitted. Of the 16 rate constants and the five quantum yields (those for the complexes AR, ARA, ATA, AD, and ADA) of Scheme I, some are correlated. Thus, two of the rate constants (we chose k_{-6} and k_{-7}) can be expressed by the following mathematical relationship:

$$k_{-6} = k_6(k_{-5}k_{-3}k_1)/(k_5k_3k_{-1})$$
$$k_{-7} = k_7(k_{-6}k_{-4}k_2)/(k_6k_4k_{-2}) \quad (2)$$

Similarly, the global equilibrium dissociation constants K_{G1} and K_{G2} of the monoliganded and diliganded complexes are related as follows (Prinz & Maelicke, 1983b; Prinz & Maelicke, 1986) to some of the rate constants:

$$2/K_{G1} = k_1/k_{-1} + k_3/k_{-3}$$
$$1/K_{G2} = k_2/k_{-2} + k_4/k_{-4} + \alpha/\beta \quad (3)$$

A similar relation exists between the global relative quantum yields Q_1 and Q_2 obtained from our equilibrium binding studies (Covarrubias et al., 1986) and the individual relative quantum yields of the individual complexes Q_{AR}, Q_{ARA}, Q_{ATA}, Q_{AD}, and Q_{ADA}:

$$Q_{AD} = K_{D3}[Q_1(1/K_{D1} + 1/K_{D3}) - Q_{AR}/K_{D1}]$$
$$Q_{ADA} = K_{D3}K_{D4}[Q_2[1/(K_{D1}K_{D2}) + 1/(K_{D3}K_{D4}) + \beta/(K_{D1}K_{D2}\alpha)] - Q_{ARA}/(K_{D1}K_{D2}) - Q_{ATA}\beta/(K_{D1}K_{D2}\alpha)] \quad (4)$$

(K_{Di} denotes an individual equilibrium constant, i.e., k_{-i}/k_i.)

RESULTS AND DISCUSSION

Basic Data Set. Figure 1 exemplifies the kinetics of association of NBD-5-acylcholine and of [^{3}H]acetylcholine to the membrane-bound nicotinic acetylcholine receptor from *T. marmorata* measured by two different assays, fluorescence stopped-flow (dotted curves), and rapid filtration (crosses and plus signs). Because the kinetics extend over several orders of magnitude in time, two time ranges are shown (with only the stopped-flow kinetics extending to the subsecond time range). To allow comparison of the three data sets, ligand concentrations and fluorescence are given in relative values, setting the concentration (fluorescence) immediately after mixing as 100% and that after 30 min of incubation as 0%. This type of display was used for the following reason: While for the filtration assays the free ligand concentration can be easily obtained from the radioactivity or fluorescence of the filtrate, the same is very difficult to achieve for the stopped-flow kinetics, as it requires knowledge of the quantum yields of free and bound fluorescent ligand. In contrast to binding to the solubilized nAChR from *Electrophorus electricus* (Prinz & Maelicke, 1983a) (which is accompanied by complete quenching of the ligand's fluorescence), binding to membrane-bound nAChR from *T. marmorata* is accompanied by only partial quenching (Covarrubias et al., 1986). As different

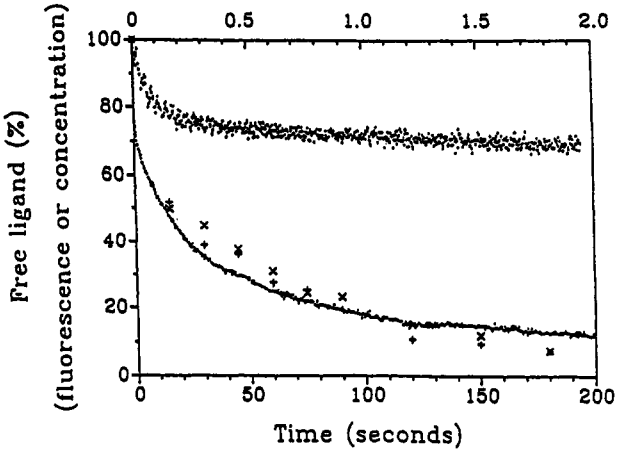

FIGURE 1: Association kinetics of NBD-5-acylcholine and of [^{3}H]acetylcholine to membrane-bound nAChR from *Torpedo marmorata* electrolytes. (●) 200 nM NBD-5-acylcholine and 200 nM (in terms of ACh binding sites) *Torpedo* membrane fragment (TMF) were rapidly mixed at a ratio of 1:1 in a stopped-flow spectrofluorimeter. Fluorescence was recorded and calibrated taking the level immediately after mixing as 100 and the value obtained after 30 min as 0. Data are displayed in two time ranges: (upper curve) 0–2 s with 2-ms time resolution; (lower curve) 0–200 s with 200-ms time resolution. (×) 200 nM NBD-5-acylcholine and 200 nM TMF were mixed by vortexing to a concentration of 100 nM each, the reaction mixture was filtered through Whatman GF/C filters at the indicated times, and the fluorescence of aliquots of the filtrate was measured in a quantum counting fluorimeter. 100% fluorescence refers to the value recorded in the presence of a large excess (10^{-4} M) of acetylcholine. Fluorescence after 30 min was taken as 0. Time range: 0–200 s. (+) 200 nM [^{3}H]acetylcholine and 200 nM TMF were mixed and filtered as above, and the radioactivity of filtrate aliquots was determined at the indicated times. The experiment was calibrated by taking the radioactivity determined in a separate experiment in the presence of 10^{-4} M acetylcholine as 100 and the radioactivity recorded after 30 min as 0. Time range: 0–200 s. The kinetics were performed at 22 °C.

ligand–nAChR complexes are passed in the course of an association reaction the fluorescence amplitudes are combinations of different quantum yields and thus cannot be translated easily into concentrations. As a first approximation, however, the data from the filtration assays appear sufficiently similar to those from the stopped-flow kinetics (Figure 1) so as to justify this simplified concentration calibration of fluorescence for the extraction of initial rate constants of association and dissociation (see below).

The kinetics of association (Figure 1) clearly were biphasic (Covarrubias et al., 1984), with approximately 20–25% of the signal in the subsecond time range. The majority of the signal developed much slower, with a half-life of approximately 20 s. Similar results have previously been reported by others (Heidmann & Changeux, 1979; Dunn et al., 1980; Boyd & Cohen, 1980) and have been interpreted as evidence for a preexisting equilibrium between two states of the nAChR, one with low affinity and the other with high affinity for agonist.

As the most unbiased means of extracting the rate constant of association from the rapid phase (Prinz, 1991), we performed stopped-flow association kinetics at different concentrations of receptor and ligand, determined the initial velocities (from the slopes at zero time), and plotted them versus the concentration of the reaction partner the concentration of which was varied. A linear relationship was found which is expected for a reaction of second order. From the slope, a second-order rate constant of 6.3×10^6 M^{-1} s^{-1} was deduced. It must be considered a lower limit for the following two reasons: (i) It is based on the assumption of complete quench-

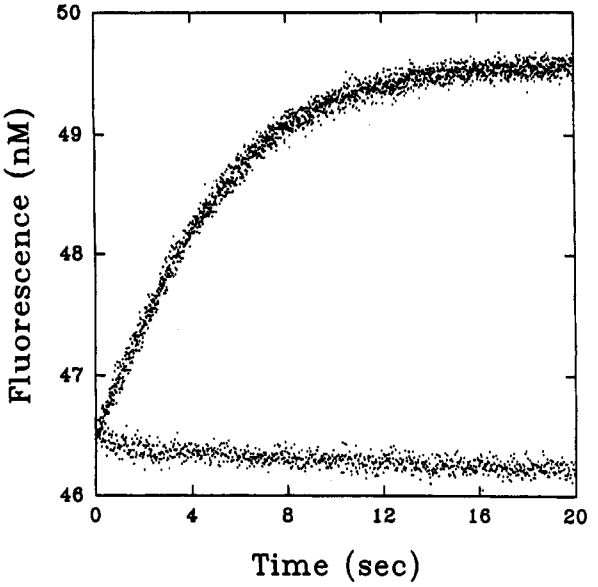

FIGURE 2: Dissociation kinetics of preformed NBD-5-acylcholine–receptor complexes after rapid mixing with a high concentration of acetylcholine. 100 nM NBD-5-acylcholine and 100 nM TMF were incubated for 30 min prior to rapid mixing (1:1) with either standard buffer (lower trace) or 10 or 100 μM ACh in standard buffer (two superimposed upper traces). From the corresponding half-logarithmic plot, a first-order rate constant of 0.2 s^{-1} was deduced. The kinetics were performed at 22 °C.

ing of the fluorescence of bound ligand. As shown previously (Covarrubias et al., 1986), this does not apply to membrane-bound nAChR from *Torpedo*. (ii) It is based on the assumption that both ligand-binding sites per receptor molecule participate in this reaction step. As will be shown below, only approximately 20% of all receptor binding sites (those in the D conformation) participate in the initial rapid reaction step (so that a 5-fold higher value is used in the actual fitting procedure, see below).

The kinetics of dissociation of NBD-5-acylcholine–nAChR complexes were studied after rapid mixing with a large excess of acetylcholine (Figure 2). The corresponding half-logarithmic plots were practically linear yielding a rate constant of 0.2 s^{-1}. In noteworthy contrast to our previous studies of the nAChR from *E. electricus* (Prinz & Maelicke, 1983b), the dissociation kinetics did not slow down when the concentration of acetylcholine was further increased. This suggests a random mechanism of ligand–nAChR complex dissociation for the *Torpedo* receptor.

Beyond the Basic Data Set. So far we have dealt with the extraction of a few basic properties of ligand interaction of the *Torpedo* nAChR, thereby avoiding any assumptions as to a reaction scheme. In contrast, the following experiments were explicitly aimed at identifying a suitable reaction scheme to be employed in an extensive numerical data analysis. To avoid any assumptions as to the fluorescence quantum yields of ligand–receptor complexes, we began with kinetic studies using radioactively labeled probes.

Figure 3a representatively shows the kinetic patterns of association of [^{3}H]acetylcholine to membrane-bound *Torpedo* nAChR. At low concentrations (10 nM), the reaction was so fast that it could not be resolved by the filtration assay. At ACh concentrations approximately equal to the concentration of binding sites at the nAChR (100 nM), the majority of the reaction was relatively slow (time range of minutes). At even higher ACh concentrations (500 nM), the reaction became faster again. These properties require a reaction scheme with two preexisting states and ligand-induced conformational transitions between them, i.e., a scheme such as Scheme I: (i) At low agonist concentrations, all ligand will bind to the high-affinity state of free receptor (D state), resulting in very rapid association kinetics. (ii) At ligand concentrations near the receptor concentration, some but not all ligand will bind rapidly to the preexisting D state. The remaining ligand will distribute between the low-affinity R state and newly formed D state. The latter can be formed directly from unliganded receptor (R → D in Scheme I) or by means of a conformational change from liganded receptor (mainly AR → AD in Scheme I). Clearly, the total reaction will be slower than when only the preexisting D state is occupied. (iii) Because only the path via AR is a reaction of second order, the increased rate of association at high ligand concentration (Figure 3a) indicates that this path dominates the reaction under the experimental conditions applied.

Figure 3b shows kinetics of association of [^{3}H]ACh to *Torpedo* nAChR preincubated with unlabeled ACh. The reaction proceeded faster to completion than without preincubation, which is consistent with the idea that the dominating form in equilibrium of monoliganded receptor is AD.

Further insight into the effect of preincubation of ligand association to membrane-bound nAChR can be obtained by time-resolved kinetics. For this purpose, NBD-5-acylcholine was used as the monitoring ligand, and the kinetics are displayed on a logarithmic time scale. As shown in Figure 3c, preincubation with acetylcholine caused a decrease in the rate of the first phase and an increase in the rate of the second phase of NBD-5-acylcholine association. The decrease in initial rate, in the presence of acetylcholine, is due to competition for the same binding sites. The increase in rate in the subsequent phase corresponds to the data shown in Figure 3b and to the explanation given above.

Complete Numerical Analysis of Reaction Kinetics. From the preceding results, the kinetics of ligand interaction of membrane-bound *Torpedo* nAChR require for their analysis a scheme that accounts for (i) two binding sites per receptor monomer, (ii) a preexisting equilibrium between two conformational states of the nAChR (one with high and the other with low affinity for agonist), and (iii) ligand-induced shifts of this equilibrium. To accommodate the electrophysiological data available, an additional conformational state (the ion-translocating state) must be considered. Scheme I is the minimal reaction mechanism that agrees with these conditions. It therefore formed the basis of the numberical analysis of the data shown in Figures 3 and 4.

The 16 rate constants of Scheme I and the quantum yields of complexes AR, ARA, ATA, AD, and ADA bring up to 21 the total number of parameters to be fitted. Equation 2 reduces the number of unknowns to 19. The number of parameters can be further reduced to 15 by taking into account the results from equilibrium binding studies and eqs 4 and 5. The observation of approximately 20% rapid association [Figure 1 and Heidmann and Changeux (1979)] sets the ratio R/D (i.e., $k_{-5}/k_5 = K_{D5}$) to 5.0. The remaining 14 parameters were further reduced to eight by taking the rate constants involved in the reaction path R–AR–ARA–ATA from published electrophysiological experiments (Sine & Steinbach, 1987). The remaining eight unknowns are the rate constants k_3, k_4, k_5, k_6, and k_7 and the relative quantum yields Q_{AR}, Q_{ARA}, and Q_{ATA}.

Even with this reduced number of parameters, the selection of the initial parameters is crucial for the quality of the final fits. For the NBD-5-acylcholine kinetics, we took as initial parameters identical values for the on-rate k_3 and k_4, i.e.,

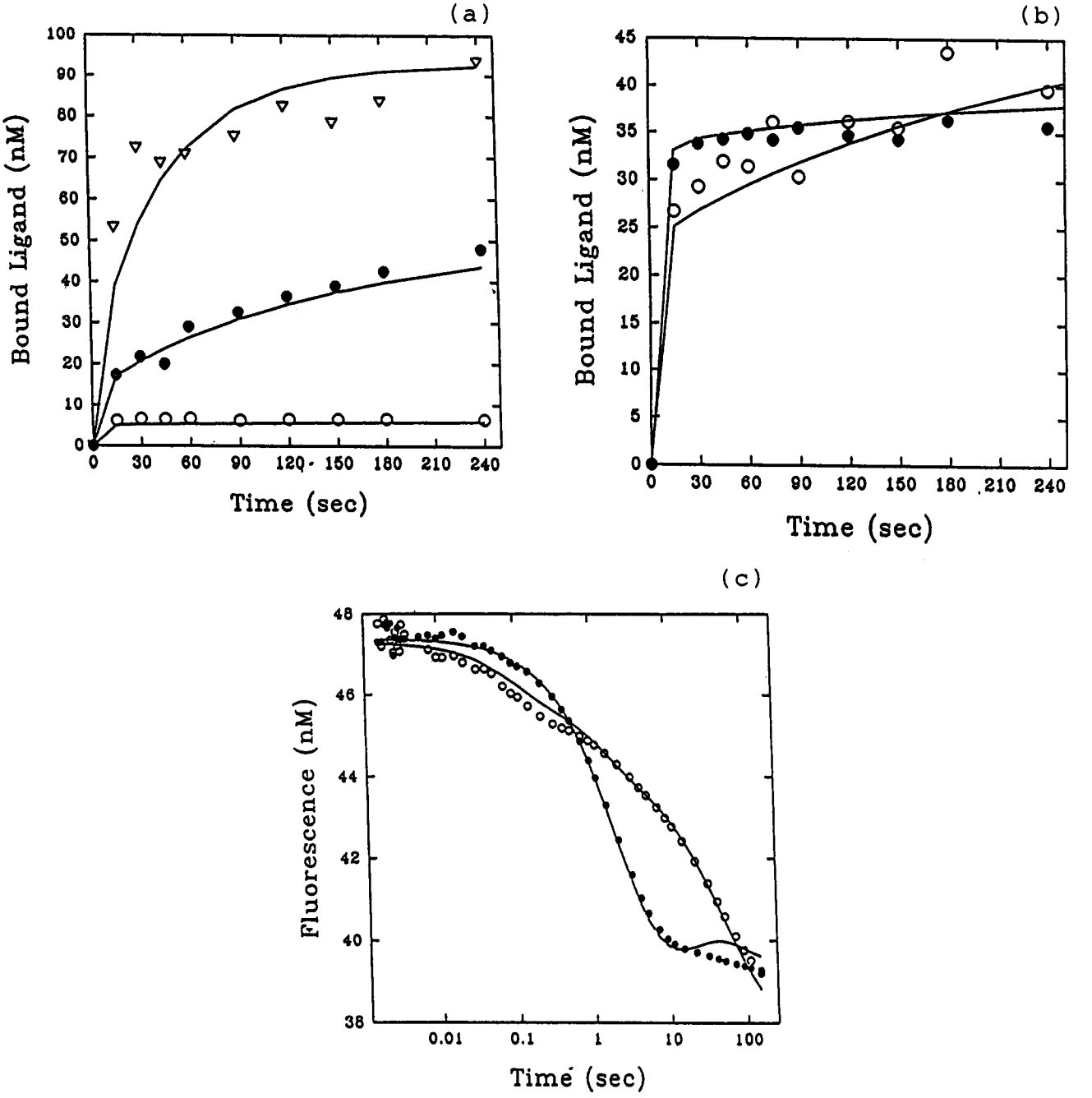

FIGURE 3: Kinetics of dissociation of [^{3}H]acetylcholine and of NBD-5-acylcholine to membrane-bound *Torpedo* nAChR under different experimental conditions. (a) Kinetics of association of [^{3}H]acetylcholine. (○) 10, (●) 100, and (▽) 500 nM [^{3}H]acetylcholine were mixed with 100 nM TMF, and the reaction mixture was filtered through glass-fiber filters as described above. The concentration of bound ligand was calculated from the radioactivity in the filtrate according to eq 1. [Note that the statistical error increases with increasing ligand concentrations because bound ligand is calculated from the difference between total and free ligand concentration (eq 1)]. (b) Effect of preincubation with acetylcholine on the kinetics of association of [^{3}H]acetylcholine. 100 nM TMF was incubated with (○) 0 and (●) 100 nM nonradioactive acetylcholine for 30 min prior to the addition of 100 nM [^{3}H]acetylcholine. All other conditions as described for panel a. (c) Effect of preincubation with acetylcholine on the kinetics of association of NBD-5-acylcholine. 100 nM TMF was incubated with (○) 0 and (●) 100 nM acetylcholine for 30 min. The mixture was transferred into a stopped-flow fluorimeter and was rapidly mixed (1:1) with 100 nM NBD-5-acylcholine. The decrease in fluorescence versus time is shown in a logarithmic time scale. Each record is the average of 24 experiments (four time ranges; eight experiments for the shorter and four experiments for the longer time ranges). The solid lines represent theoretical curves calculated on the basis of the parameters of Table II. The kinetics were performed at 22 °C.

$k = 3 \times 10^7$ M^{-1} s^{-1}, which is the lower limit of the rate constant of initial association. Similarly, the rate constants k_5, k_6, and k_7 were set to the same numerical value of 0.003 s^{-1}, i.e., to the rate constant of the slow phase of the association kinetics, as obtained by two-exponential fits of experiments such as shown in Figure 3a. The same initial values were also used for the acetylcholine kinetics, because of the similarity of the association reactions of ACh and NBD-5-acylcholine (Figure 1).

Numerical fitting was performed with the program FACSIMILE (for details see Materials and Methods. After each round of curve fitting, all parameters were varied in order to find a better fit for the data set. These variations took into account that some of the parameters are correlated. For example, a decrease in the equilibrium dissociation constant K_{G1} causes a similar effect as a decrease in the quantum yield Q_1, namely, a reduction in the final level of fluorescence in a certain concentration range. Consequently, in such cases

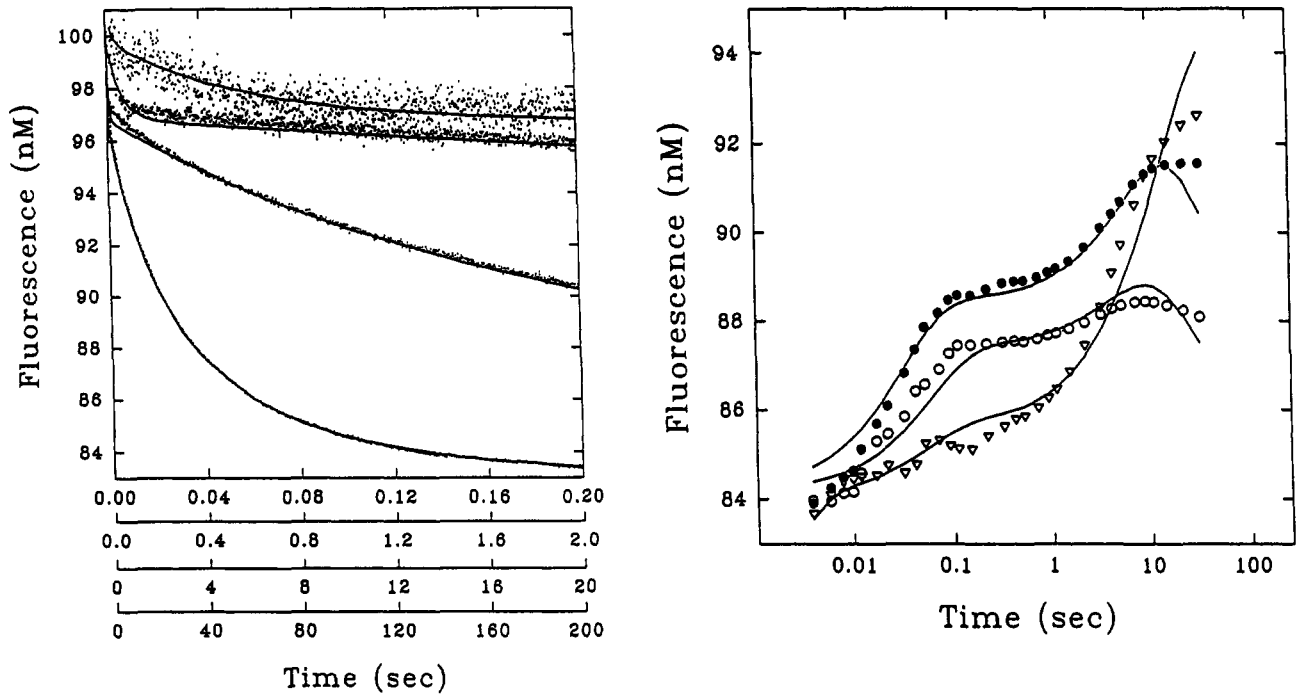

FIGURE 4: Kinetics of association to and dissociation from *Torpedo* nAChR of NBD-5-acylcholine. (a, left) Association kinetics. Equal volumes of 200 nM (in terms of ACh binding sites) TMF and 200 nM NBD-5-acylcholine were rapidly mixed 1:1 in a stopped-flow fluorimeter, and the decrease in fluorescence was recorded as a function of time. Four different experiments recorded at four overlapping time ranges (from top to bottom) are shown. These were 1.5–200 ms (eight experiments were averaged), 1.5–2000 ms (eight experiments), 1.5–20 000 ms (four experiments), and 1.5–200 000 ms (four experiments), respectively. The time constants for the four experiments were 0.1, 1, 10, and 50 ms, respectively. (b, right) Dissociation of preformed NBD-5-acylcholine–receptor complexes. 100 nM NBD-5-acylcholine and 100 nM membrane-bound receptor were incubated for 30 min, transferred into the syringe of a stopped-flow fluorimeter, and rapidly mixed (1:1) with either (●) 200, (○) 500, or (▽) 1000 nM acetylcholine. The observed increase in fluorescence is plotted in a logarithmic time scale. The kinetics were performed at 22 °C. The solid lines represent theoretical curves calculated with the parameters listed in Table II.

only one but not the other of a pair of correlated parameters was varied. As a general rule, each on-rate is correlated with the off-rate of the same reaction step, while there is no such strong correlation between on-rates and the corresponding equilibrium dissociation constants.

To exemplify our approach, we varied the global equilibrium dissociation constants K_{G1} and K_{G2} of eq 3 [known from equilibrium studies (Covarrubias et al., 1986; Fels et al., 1982)] rather than the individual ones. In this way, an additional control of the fitting procedure was achieved in that unreasonable combinations of parameters were avoided. For the acetylcholine kinetics, the equilibrium constants K_{D1} and K_{D2} of the complexes AR and ARA were taken from electrophysiological studies (Sine & Steinbach, 1987). For the NBD-5-acylcholine kinetics, the dissociation rate constants k_{-1} and k_{-2} were assumed equal to those observed for acetylcholine (Sine & Steinbach, 1987), and k_1 and k_2 were varied. The equilibrium dissociation constants of the desensitized conformations, K_{D3} and K_{D4}, were calculated using eq 3. The same reasoning was applied to the variation of the relative quantum yields. Again, relative quantum yields of the first (Q_1) and second (Q_2) binding site [known from equilibrium studies (Covarrubias et al., 1986)] were varied in addition to Q_{AR}, Q_{ARA}, and Q_{ATA}. Equation 4 was used for the calculation of the quantum yields Q_{AD} and Q_{ADA} of the desensitized conformations. In the described way, we tried to include into the numerical fitting procedure as much solid information as possible from the large body of biochemical and physiological data already available for *Torpedo* nAChR.

All these attempts would not have led to significant values for the parameters involved if only single experiments were fitted. Instead, we simultaneously fitted whole sets (128 experiments) of equilibrium binding experiments, rapid filter kinetics, and fluorescence kinetics. The majority of these (80) were association kinetics with NBD-5-acylcholine measured at different concentrations of ligand (25, 50, 100, and 200 nM) and receptor (5, 25, 50, 100, and 500 nM) and at four different time ranges each. In addition, the interdependence of the data sets for acetylcholine and NBD-5-acylcholine (e.g., Figure 3c) was taken into account. As an example, the relative quantum yields of individual NBD-5-acylcholine-nAChR complexes were obtained with the help of K_{D5}, which was obtained from the data displayed in Figure 3a.

The rate and equilibrium constants obtained from the fitting procedure are given in Table I. The relative error margins for each parameter indicated therein are the 5% and 95% confidence levels obtained from the statistical analysis of the fitting algorithm assuming that all other parameters are constant. Table II lists all rate and equilibrium constants of Scheme I independent of whether they were determined by our fitting procedure, by further calculation (see Materials and Methods), or whether they were obtained from other sources.

The Effect of the Membrane Environment on nAChR Kinetics. The biphasic association kinetics depicted in Figures 1 and 4a are typical for membrane-bound *Torpedo* nAChR. In contrast, when the receptor was solubilized, the associate rate increased, resulting in a complete loss of the slow phase of the usual kinetic pattern. As shown in Figure 5 by the results of rapid filtration experiments, a comparable large increase in the rate of ACh association to membrane-bound nAChR was obtained when the membrane structure was modified by the addition of nonionic detergents or alcohols (Boyd & Cohen, 1984), membrane-motility agents (Kosower et al., 1977), or by phospholipase treatment. As would be expected, the effect of ethanol treatment was reversed by

Table I: Rate and Equilibrium Constants Derived by Numerical Fitting to Scheme I of Our Set of Experimental Data[a]

parameter	ligand	
	NBD-5-acylcholine	acetylcholine
k_1 (M^{-1} s^{-1})	2.9 (2.8–3.0) × 10^8	
k_2 (M^{-1} s^{-1})	3.9 (1.6–9.5) × 10^5	
k_3 (M^{-1} s^{-1})	1.9 (1.7–2.2) × 10^8	1.4 (1.0–2.0) × 10^8
k_4 (M^{-1} s^{-1})	6.4 (5.8–6.9) × 10^6	9.5 (7.5–12.0) × 10^7
k_5 (s^{-1})	5.5 (1.4–21.2) × 10^{-4}	5.5 (1.4–21.2) × 10^{-4}
k_6 (s^{-1})	0.79 (0.78–0.81)	13.2 (1.8–96.6)
K_{D5}	4.9 (4.75–5.05)	4.9 (4.75–5.05)
K_{G1} (M)	1.2 (1.1–1.3) × 10^{-8}	4.5 (4.0–5.0) × 10^{-8}
K_{G2} (M)	5.1 (4.8–5.3) × 10^{-9}	3.1 (2.8–3.5) × 10^{-8}

[a] The values in parentheses denote the 5% and 95% confidence levels obtained by fitting the particular constant with all other parameters invariant. k_{-1}, k_{-2}, α, and β (for all ligands) and k_1 and k_2 (for acetylcholine) were taken (uncorrected for any differences in experimental conditions) from published electrophysiological studies (Sine & Steinbach, 1987). The global equilibrium dissociation constants relate to the individual equilibrium dissociation constants according to eq 1. For the quantum yields (relative to the quantum yield of NBD-5-acylcholine in standard buffer) of the individual complexes, the following values were obtained: Q_{NR} = 40% (38–42), Q_{ARN} = 16% (13–20), Q_{NRA} = 750% (340–1600), Q_{NTN} = 460% (170–1200), Q_{ATN} = 7700% (800–70 000), Q_{NTA} = 160% (120–210), Q_{ADN} = 17% (14–20), Q_{NDA} = 142% (137–147), Q_1 = 60.7% (59.5–62.0), Q_2 = 80.0% (79.8–80.2). The values in parentheses denote the confidence limits. The equilibrium quantum yields Q_1 and Q_2 relate to the individual values according to eq 3. N denotes NBD-5-acylcholine and A denotes acetylcholine, so that Q_{ADN} is the quantum yield of the desensitized receptor to which acetylcholine was bound first and NBD-5-acylcholine was bound second. Neither the quantum yield Q_{NRN} nor the rate constant k_7 could be determined reliably by data fitting, and thus they were set to 1400(%) for Q_{NRN}, and to 14.5 and 2.3 s^{-1}, respectively, for k_7 for NBD-5-acylcholine and acetylcholine.

Table II: Rate and Equilibrium Constants of Scheme I[a]

parameter	ligand	
	NBD-5-acylcholine	acetylcholine
K_{D1} (M)	1.7 × 10^{-6}	5.0 × 10^{-5} (+)
k_1 (M^{-1} s^{-1})	2.9 × 10^8	1.0 × 10^7 (+)
k_{-1} (s^{-1})	500 (+)	500 (+)
K_{D2} (M)	2.6 × 10^{-3}	1.0 × 10^{-5} (+)
k_2 (M^{-1} s^{-1})	3.9 × 10^5	1.0 × 10^8 (+)
k_{-2} (s^{-1})	1000 (+)	1000 (+)
K_{D3} (M) (*)	1.2 × 10^{-9}	4.6 × 10^{-9}
k_3 (M^{-1} s^{-1})	1.9 × 10^8	1.4 × 10^8
k_{-3} (s^{-1})	0.23	0.64
K_{D4} (M) (*)	1.0 × 10^{-8}	6.2 × 10^{-8}
k_4 (M^{-1} s^{-1})	6.4 × 10^6	9.5 × 10^7
k_{-4} (s^{-1})	0.064	5.9
K_{D5}	4.9	4.9
k_5 (s^{-1})	5.5 × 10^{-4}	5.5 × 10^{-4}
k_{-5} (s^{-1})	2.7 × 10^{-3}	2.7 × 10^{-3}
k_6 (s^{-1})	0.79	13.2
k_{-6} (s^{-1}) (*)	2.7 × 10^{-3}	5.9 × 10^{-3}
k_7 (s^{-1})	14.5	2.3
k_{-7} (s^{-1}) (*)	1.9 × 10^{-7}	6.4 × 10^{-6}
α (s^{-1})	35 (+)	35 (+)
β (s^{-1})	480 (+)	480 (+)
K_{G1} (M)	1.2 × 10^{-8}	4.5 × 10^{-8}
K_{G2} (M)	5.1 × 10^{-9}	3.1 × 10^{-8}

[a] The listed parameters either were obtained by our data analysis (see Table I), were calculated from these values according to eqs 2 and 3 (*), or were taken from published electrophysiological studies (Sine & Steinbach, 1987) (+). The latter were obtained at 11 °C, while all our experiments were performed at 22 °C.

appropriate dilution with buffer, whereas the effect of phospholipase treatment was irreversible at all experimental conditions applied.

The effect of ethanol on the association kinetics of NBD-5-acylcholine was studied in more detail (Figure 6). As is particularly well demonstrated in logarithmic time scale, the slow phase of the kinetics gradually disappeared as the ethanol concentration was increased. In parallel, the point of inflection of the slow phase was gradually shifted toward

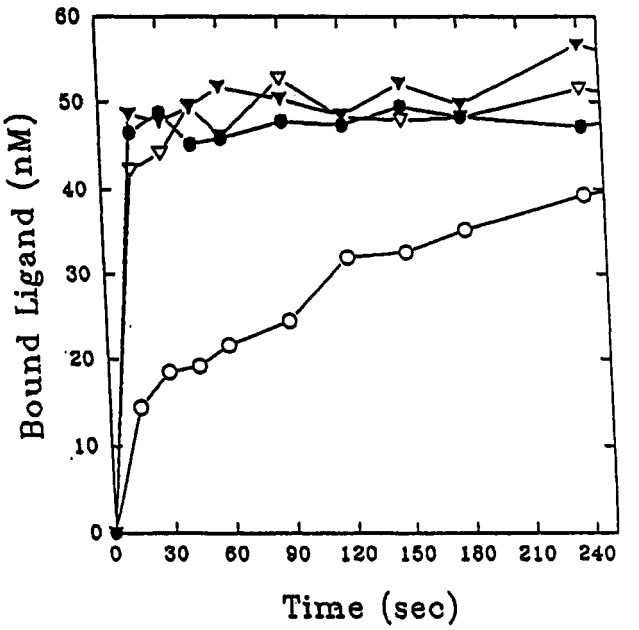

FIGURE 5: Kinetics of association of [^{3}H]acetylcholine to modified *Torpedo* membrane fragments. 100 nM [^{3}H]acetylcholine was added to 100 nM TMF, and the kinetics of association were measured as before by the filtration assay. (○) Control, i.e., TMF in standard buffer; (●) TMF were treated for 30 min with 0.01% A_2C, prior to the addition of [^{3}H]acetylcholine; (▽) TMF were treated for 30 min with 0.01% Tween 80 prior to the addition of [^{3}H]acetylcholine; (▼) TMF were treated with 10 units of phospholipase D for 2 h, followed by three washes (by repeated centrifugation), prior to the addition of [^{3}H]acetylcholine.

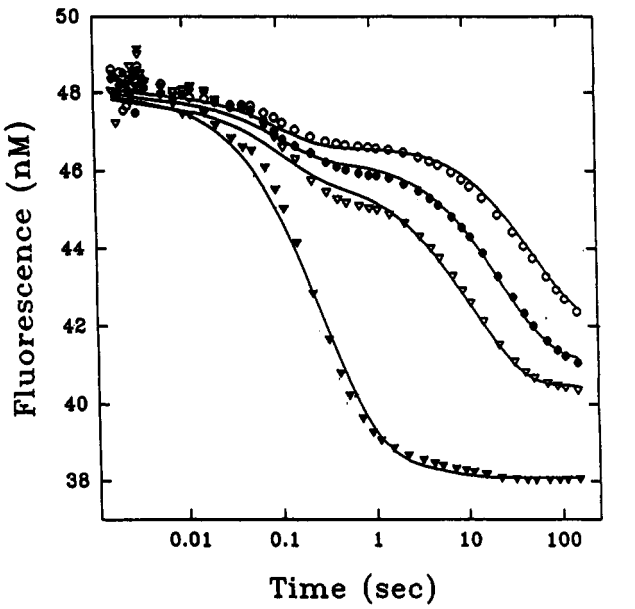

FIGURE 6: Effect of ethanol on the association kinetics of NBD-5-acylcholine to membrane-bound nAChR. 100 nM NBD-5-acylcholine in standard buffer containing (○) 0%, (●) 2%, (▽) 4%, and (▼) 20% (v/v) ethanol were rapidly mixed 1:1 with 100 nM TMF, and the change in fluorescence versus time was recorded. The solid lines represent theoretical curves calculated with the parameters listed in Table I, except that for the experiments in the presence of ethanol k_6 was changed to 1.9, 4.0, and 100 s^{-1}, respectively. In addition, the amplitudes were adjusted using for Q_1 and Q_2 the following values at the given ethanol concentrations: 0.6 and 0.85, 0.54 and 0.85, and 0.52 and 0.76, respectively. The experiments were performed at 22 °C.

shorter times, with the total amplitude remaining almost constant. Because the point of inflection in a logarithmic time scale is inversely related to the rate constant of an exponential decay curve, the observed shift is equivalent to an acceleration in the presence of ethanol, of the slow phase of the association reaction. This finding was further quantified by numerical fitting: Only the rate constant k_6 needed to be varied (always together with the global relative quantum yields Q_1 and Q_2, because these are very sensitive to the presence of organic solvent), in order to obtain an adequate fit of the data. In contrast, the variation of other parameters, e.g., K_{D5}, did not produce parameter sets that appropriately fitted the experimental data. This finding strongly suggests that ethanol (and by inference also the other membrane structure disturbing compounds tested) increased the rate of conformational transition from AR to AD (possibly generally from the R state to the D state of the receptor), which is consistent with previous biochemical and electrophysiological findings (Weiland & Taylor, 1979; Boyd & Cohen, 1984; Ogden et al., 1981). It also agrees with the kinetics of solubilized (purified) nAChR from *E. electricus* which are characterized by rapid transitions from AR to AD and from ARA to ADA (Prinz & Maelicke, 1983b).

GENERAL DISCUSSION

The Reaction Scheme. Quantitative analysis of the type shown here critically depends on the reaction scheme employed. Scheme I was used because it agreed on a qualitative level with the concentration dependence of the association kinetics of [^{3}H]ACh (Figure 3a and related experiments with NBD-5-acylcholine) and the effect of agonist preincubation on [^{3}H]ACh kinetics (Figure 3b,c). In addition, it considers two binding sites per receptor monomer, a preexisting equilibrium between two states of the nAChR, and ligand-induced transitions between receptor states. All these are basic requirements for any model of the *Torpedo* receptor's mechanism of ligand interaction. An earlier scheme developed for the study of desensitization (Katz & Thesleff, 1957) properly describes the biphasic nature of the association reaction (Boyd & Cohen, 1980) but considers only *one* binding site per receptor monomer. Extensions of this scheme, including three (Heidmann & Changeux, 1979) or even four (Heidmann & Changeux, 1980) conformational states of the receptor did not suffice to appropriately fit the experimental data depicted in Figure 3a,b. Clearly, the assumption of *two* binding sites per nAChR monomer is a strict requirement for a proper fit of the data. Another strict requirement was the existence of two states of free nAChR, which excluded our earlier reaction scheme (Prinz & Maelicke, 1983b) derived for the purified nAChR from *E. electricus*. In noteworthy contrast, the inclusion in Scheme I of the complex ATA was insignificant, as its kinetic constants did not decisively affect the reaction steps controlling ligand binding, i.e., transitions 1, 3, 4, and 6 (see below).

Derived Rate and Equilibrium Constants. Within the frame provided by reaction Scheme I, the individual rate constants were obtained from simultaneous fits of a large set of independent experiments performed under identical experimental conditions. The most reliable rate constants obtained in this way are those controlling the initial phase of the association kinetics of NBD-5-acylcholine, i.e., k_3 and k_4. In contrast, k_1, k_5, and k_6 are correlated to each other, therefore excluding the extraction of independent values for them. k_7 was so little defined by our experimental data that we finally decided to set it to a fixed value (see Table I).

The equilibrium dissociation constants K_{G1} and K_{G2}, being basically those of the desensitized states AD and ADA, are well defined by our experimental data. They did not depend on the values for the other parameters, except for a marginal dependence on the relative quantum yields Q_1 and Q_2. In contrast, the K_D values of the complexes AR and ARA for NBD-5-acylcholine rather sensitively depended on the quantum yields of these complexes.

In the case of the acetylcholine kinetics, the rate constants k_1, k_{-1}, k_2, k_{-2}, α, and β were taken from published electrophysiological data on the nAChR from BC3H-1 cells (Sine & Steinbach, 1987). These data conformed reasonably well with our own set of binding and kinetic data while those obtained with ectopically expressed *Torpedo* nAChR (Sine et al., 1990) did not. Several alternative explanations may account for this disconcerting finding: (i) We cannot fully exclude a wrong local minimum of our data fit. As most of our own experiments are dominated by the transition from resting to desensitized state of liganded nAChR (the slow component of the association kinetics), which proceeds mainly via AR, the numerical value of K_{D1} is particularly crucial for the data fit. Unfortunately, K_{D1} is not well accessible by binding studies, as the complex AR only marginally contributes to the total set of ligand–nAChR complexes in equilibrium. To illustrate the limiting properties of K_{D1}, a 10-fold lower value for K_{D1} than given in Table II completely destroyed the consistency of the set of fitted parameters. (ii) It is in the nature of electrophysiological experiments that all their data on ligand binding are only inferred from the analysis of the active (ion-translocating) state(s). This is the conformational state that is least accessible by our binding studies. The fact that the ligand-binding data obtained by electrophysiological measurements with BC3H-1 nAChR agreed better with our results than those obtained with ectopically expressed *Torpedo* nAChR therefore should not be overstressed. (iii) As a further possibility, differences in posttranslational processing of the nAChR, or in plasma membrane structure, or both, in mouse fibroblasts as compared to *Torpedo* electrocytes may introduce differences also in the kinetics of the nAChR channel.

Although the set of parameters given in Table I certainly is not the only combination that fits our data, it contains some rate and equilibrium constants that do not permit much variation. This is indicated by the confidence limits given for each parameter determined. For example, the accuracy in the determination of k_6 is very high. As discussed before, the concentration dependence of the association kinetics requires that k_6 is much larger than k_5 (three orders of magnitude according to our data fit), so that under the experimental conditions described here, the ligand-induced transition from the resting to the desensitized state of the nAChR proceeds almost exclusively from AR to AD. As a consequence, k_5 is determined with a rather large error range. A similar reasoning applies for all rate constants involved in the formation and dissociation of ARA. Since binding under our experimental conditions applied proceeds mainly via AR leading to the formation of AD and ADA, the rate constants k_2, k_{-2}, and k_7 are determined with very limited accuracy.

The Role of the Membrane. As shown by the data depicted in Figures 5 and 6, the nature of the membrane environment crucially affects the kinetics of ligand interaction of membrane-bound nAChR. Although this has been observed before by others (Boyd & Cohen, 1984; Forman et al., 1989), our stopped-flow data now pinpoint the effects of organic solvents, detergents, membrane-motility agents, and phospholipase treatment to the rate of transition of AR to AD, i.e., the

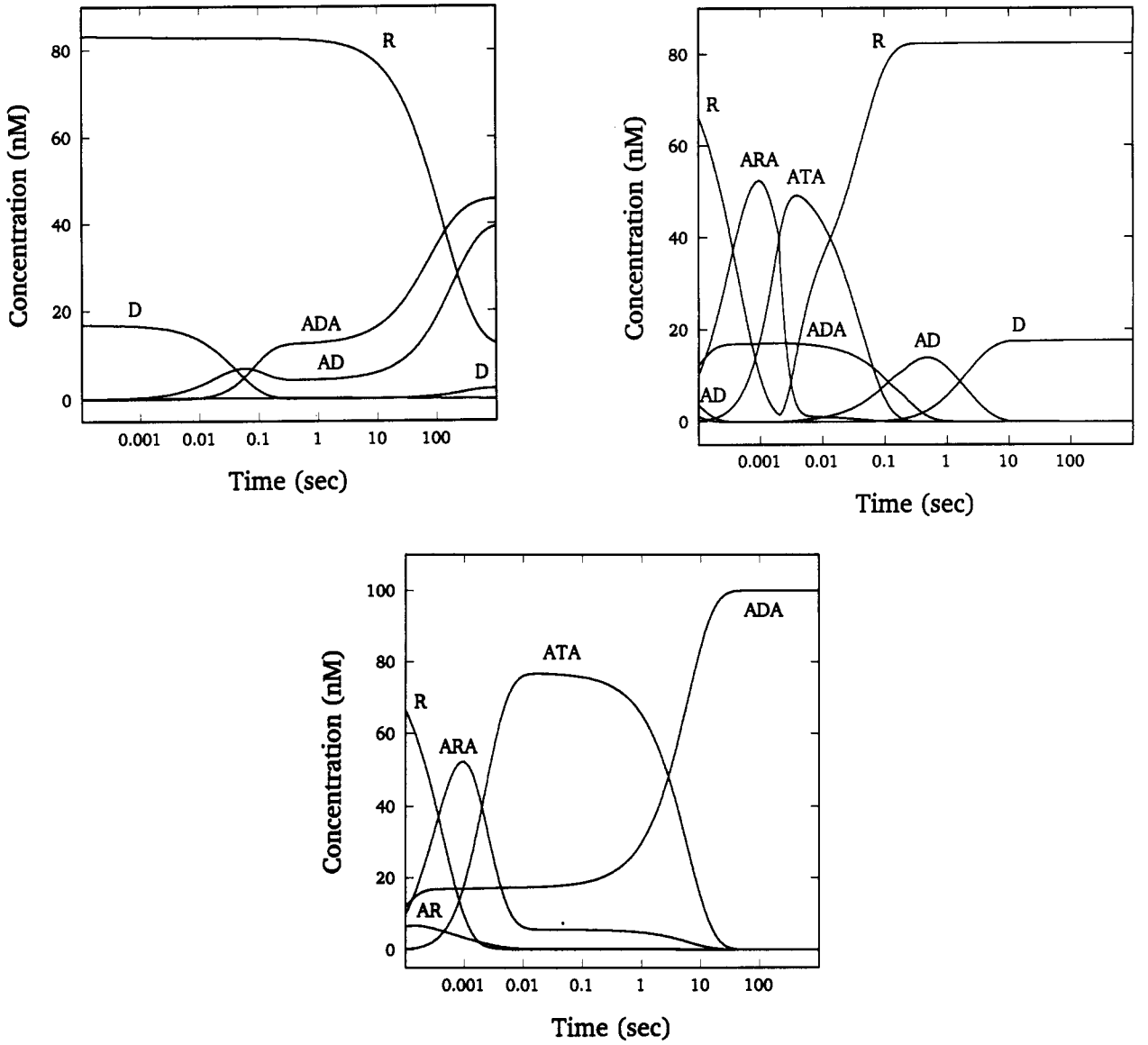

FIGURE 7: Simulations of formation and breakdown kinetics of individual acetylcholine–receptor complexes in the course of association to membrane-bound nAChR. The theoretical curves shown were calculated on the basis of reaction Scheme I and the rate constants for acetylcholine given in Table II. The notation of Scheme I is used with respect to the ligand–nAChR complexes. The concentrations (total concentrations at zero time) considered are 100 nM *Torpedo* nAChR for all three simulations and (a, top left) 200 nM acetylcholine, applied at zero time and kept for the entire period of time indicated, (b, top right) 225 μM acetylcholine (Nishi et al., 1967), applied at zero time and withdrawn after 2 ms (box function), and (c, bottom) 225 μM acetylcholine, applied at zero time and kept for the entire period indicated. Immediate uniform distribution of ACh was assumed. The theoretical curves may be considered simulations of the following three states of a cholinergic synapse: (a, top left) no excitation; (b, top right) strong excitatory event; (c, bottom) poisoning of the synapse following blockade of acetylcholine esterase.

reaction step carrying the main load of ligand-induced conformational change from the resting to the desensitized state of *Torpedo* nAChR. In contrast, previous studies (Boyd & Cohen, 1984; Forman et al., 1989) had attributed the effect to a shift, in favor of the high-affinity state, of the preexisting equilibrium of states. The latter assumption can be excluded for the *Torpedo* system, as the relative *amplitudes* of slow and fast component of our related experiments did not significantly change as a function of added ethanol (Figure 6).

The accelerating effect on the rate of the AR to AD transition shown in Figures 5 and 6 probably is due to a loss in native membrane structure, and thus a loss in specific receptor–membrane interaction. In agreement with this interpretation, ethanol or detergents only marginally affect the binding equilibria [Prinz and Veltel (1988), but see also Bradley et al. (1980)], which are defined by the desensitized states, whereas the association rate is dramatically increased (Figure 5).

Taken together, the fluidity of the membrane environment appears to be an essential element of control of the transition from the low-affinity liganded state AR to the thermodynamically favored high-affinity (desensitized) state AD. Compounds that increase the fluidity of the membrane, therefore, increase the rate of desensitization (Ogden et al., 1981). Consequently, the lipid composition of membranes (Fong & McNamee, 1986), fatty acids covalently attached to the nAChR (Olsen et al., 1984), and the presence of organic solvent (Aracava et al., 1991) have modulating effects on nAChR kinetics.

Simulations of Excitatory Events at the Cholinergic Synapse. The properties of reaction Scheme I and the reaction parameters in Table II become evident when the events occurring in the course of excitatory events at the cholinergic

synapse (neuromuscular junction or electrolyte synapse) are simulated. In the simulations depicted in Figure 7, three critical concentrations of acetylcholine are considered, a low, persistent concentration of ACh, comparable to slightly elevated basal ACh levels in the synaptic cleft (Figure 7a), a high, transient concentration of ACh, comparable to an excitatory event (Figure 7b), and a high, persistent level of ACh, comparable to the phenomenon of desensitization (Figure 7c).

At low but persisting considerations of acetylcholine in the vicinity of the receptor (Figure 7a), the relative concentrations of resting and desensitized state of free nAChR are shifted slowly to a new equilibrium state defined by the basal ligand concentration. There is no significant formation of ATA (the ion-transmitting state), and thus there is no significant level of response. It is believed that 5–10-fold higher concentrations of ACh exist in the specific postsynaptic region when the minimal transient response defined by the miniature endplate potential is produced (Nishi et al., 1967). Thus, the relative concentration of nAChR in its low-affinity (resting) state defines the maximal level of response (concentration of ATA) that can be achieved, with the basal concentration of ACh in the synaptic cleft possibly serving as a regulatory signal.

In the case of a strong excitatory event caused by a short pulse of high (Nishi et al., 1967) ACh concentration (Figure 7b), the ion-translocating state ATA is rapidly formed, reaching its maximum within a few milliseconds. If the pulse rapidly decays, as is typical in the presence of active acetylcholine esterase (simulated here by the withdrawal of the pulse after 2 ms), free nAChR in its resting state is restored in the subsecond time range. Depending on the size of consecutive ACh pulses, the *Torpedo* nAChR therefore is capable of responding 10 or more times per second to an excitatory pulse (Figure 7b). Interestingly, and consistent with the physiology of the cholinergic synapse, the total concentration of desensitized nAChR (D + AD + ADA) hardly varies under these conditions.

In the case of the pathological situation of a long lasting pulse of high ACh concentration, as is typical under conditions of blocked acetylcholine esterase, the concentration of the ion-translocating state ATA remains high for a longer period of time than at usual excitatory events (Figure 7c). As ATA is consecutively transformed into ADA, there is no significant re-formation of the resting state of free nAChR, and the ability to respond is lost.

It is interesting to consider the kinetics of nAChR inactivation under the experimental conditions of Figure 7a,b. Under conditions of a short pulse of ACh, ATA rapidly decays into R, with the formation of desensitized nAChR being insignificant (Figure 7b). In contrast, under conditions of a long-lasting ACh pulse, ATA decays into desensitized nAChR forms, mainly into ADA (Figure 7c). Thus, even with the rather simple scheme applied here (Scheme I), several rate constants of inactivation must be considered.

ACKNOWLEDGMENT

Most of this work was performed while both authors were associated with the Max-Planck-Institut. The technical assistance by Martina Wischnewski and the secretarial help by Veronika Wölfle are gratefully acknowledged. We thank our colleagues Drs. Manual Covarrubias and Jürgen Kuhlmann for fruitful discussions.

REFERENCES

Aracava, Y., Froes-Ferrao, M. M., Pereira, E. F. R., & Albuquerque, E. X. (1991) *Ann. N.Y. Acad. Sci. 625*, 451–472.

Auerbach, A., & Sachs, F. (1983) *Biophys. J. 42*, 1–10.

Boyd, N. D., & Cohen, J. B. (1980) *Biochemistry 19*, 5353–5358.

Boyd, N. D., & Cohen, J. B. (1984) *Biochemistry 23*, 4023–4029.

Bradley, R. J., Peper, K., & Stern, R. (1980) *Nature 284*, 60–62.

Changeux, J.-P., & Podleski, T. (1968) *Proc. Natl. Acad. Sci. U.S.A. 59*, 944–950.

Changeux, J.-P., Llinas, R. R., Purves, D., & Bloom, F. E. (1988) in *Functional Architecture and Dynamics of the Nicotinic Acetylcholine Receptor: An Allosteric Ligand-Gated Ion Channel*, pp 21–168, Fidia Research Foundation, Neuroscience Award Lectures, New York.

Colquhoun, D., & Ogden, D. C. (1986) in *Structure and Function of the Nicotinic Acetylcholine Receptor*, (Maelicke, A., Ed.) Vol. 3, pp 197–218, NATO ASI Series H: Cell Biology, Springer Press, Berlin.

Conti-Tronconi, B. M., Diethelm, B. M., Wu, X., Tang, F., Bertazzon, R., Schröder, B., Reinhardt-Maelicke, S., & Maelicke, A. (1991) *Biochemistry 30*, 2575–2584.

Covarrubias, M., Prinz, H., & Maelicke, A. (1984) *FEBS Lett. 169*, 229–233.

Covarrubias, M., Prinz, H., Meyers, H.-W., & Maelicke, A. (1986) *J. Biol. Chem. 261*, 14955–14961.

Delcour, A. H., & Hess, G. P. (1986) *Biochemistry 25*, 1793–1799.

Dunn, S. M., Blanchard, S. G., & Raftery, M. A. (1980) *Biochemistry 19*, 5645–5652.

Dunn, S. M. J., Shelman, R. A., & Agey, M. W. (1989) *Biochemistry 28*, 2551–2557.

Fels, G., Wolff, E. K., & Maelicke, A. (1982) *Eur. J. Biochem. 127*, 31–38.

Fong, T. M., & McNamee, M. G. (1986) *Biochemistry 25*, 830–840.

Forman, S. A., Righi, D. L., & Miller, K. W. (1989) *Biochim. Biophys. Acta 987*, 95–106.

Heidmann, R., & Changeux, J.-P. (1979) *Eur. J. Biochem. 94*, 255–279.

Heidmann, R., & Changeux, J.-P. (1980) *Biochem. Biophys. Res. Commun. 97*, 889–896.

Heidmann, R., Bernhardt, J., Neumann, E., & Changeux, J.-P. (1983) *Biochemistry 22*, 5452–5459.

Jackson, M. B. (1984) *Proc. Natl. Acad. Sci. U.S.A. 81*, 3901–3904.

Jürss, R., Prinz, H., & Maelicke, A. (1979) *Proc. Natl. Acad. Sci. U.S.A. 76*, 1064–1068.

Kang, S., & Maelicke, A. (1980) *J. Biol. Chem. 255*, 7326–7332.

Karpen, J. W., Sachs, A. B., Cash, D. J., Pasquale, E. B., & Hess, G. P. (1983) *Anal. Biochem. 135*, 83–94.

Katz, B., & Thesleff, S. (1957) *J. Physiol. 138*, 63–80.

Klarsfeld, A., Devillers-Thiery, A., Giraudat, J., & Changeux, J.-P. (1984) *EMBO J. 3*, 35–41.

Kosower, E. M., Kosower, N. S., & Wegman, P. (1977) *Biochim. Biophys. Acta 471*, 311–317.

Maelicke, A., Fulpius, B. W., Klett, R. P., & Reich, E. (1977) *J. Biol. Chem. 252*, 4811–4830.

McCarthy, M. P., & Stroud, R. M. (1989) *Biochemistry 28*, 40–48.

Merlie, J. P., Sebbane, R., Gardner, S., & Lindstrom, J. (1983) *Proc. Natl. Acad. Sci. U.S.A. 80*, 3845–3849.

Meyers, H.-W., Jürss, R., Brenner, H. R., Fels, G., Prinz, H., Watzke, H., & Maelicke, A. (1983) *Eur. J. Biochem. 137*, 399–404.

Monod, J., Wyman, J., & Changeux, J.-P. (1965) *J. Mol. Biol. 12*, 88–118.

Musil, L. S., Carr, C., Cohen, J. B., & Merlie, J. P. (1988) *J. Cell Biol. 107*, 1113–1118.

Neubig, R. R., & Cohen, J. B. (1979) *Biochemistry 18*, 5464–5475.

Neubig, R. R., & Cohen, J. B. (1980) *Biochemistry 19*, 2770–2779.

Neubig, R. R., Boyd, N. D., & Cohen, J. B. (1982) *Biochemistry 21*, 3460–3467.

Nishi, S., Soeda, H., & Kohetsu, K. (1967) *J. Neurophysiol. 30*, 114–128.

Ogden, D. C., Siegelbaum, S. A., & Colquhoun, D. (1981) *Nature 289*, 596–598.

Olson, E. N., Glaser, L., & Merlie, J. P. (1984) *J. Biol. Chem. 259*, 5364–5367.

Pearce, S. F., & Hawrot, E. (1990) *Biochemistry 29*, 10649–10659.

Prinz, H. (1992) in *Receptor–Ligand Interactions, A Practical Approach* (Hulme, E., Ed.) pp 265–288, Oxford University Press.

Prinz, H., & Maelicke, A. (1983a) *J. Biol. Chem. 258*, 10263–10271.

Prinz, H., & Maelicke, A. (1983b) *J. Biol. Chem. 258*, 10273–10282.

Prinz, H., & Maelicke, A. (1986) *J. Biol. Chem. 261*, 14962–14964.

Prinz, H., & Veltel, D. (1986) *Biol. Chem. Hoppe-Seyler 369*, 1243–1251.

Sine, S. M., & Taylor, P. (1979) *J. Biol. Chem. 254*, 3315–3325.

Sine, S. M., & Taylor, P. (1982) *J. Biol. Chem. 257*, 8106–8114.

Sine, S. M., & Steinbach, J. H. (1987) *J. Physiol. 385*, 325–359.

Sine, S. M., Claudio, T., & Sigworth, F. J. (1990) *J. Gen. Physiol. 96*, 395–437.

Steinbach, J. H. (1989) *Annu. Rev. Physiol. 51*, 353–365.

Steinbach, J. H., & Ifune, C. (1989) *Trends Neurosci. 12*, 3–6.

Steinbach, J. H., Covarrubias, M., Sine, S. M., & Steele, J. (1986) in *Structure and Function of the Nicotinic Acetylcholine Receptor* (Maelicke, A., Ed.) NATO ASI Series H: Cell Biology, Vol. 3, pp 219–232, Springer Press Berlin.

Watters, D., & Maelicke, A. (1983) *Biochemistry 22*, 1811–1819.

Weber, M., & Changeux, J.-P. (1974a) *Mol. Pharmacol. 10*, 1–13.

Weber, M., & Changeux, J.-P. (1974b) *Mol. Pharmacol. 10*, 14–34.

Weiland, G., & Taylor, P. (1979) *Mol. Pharmacol. 15*, 197–212.